

## Universal stationary-phase treatment of far-wing and excimer spectral line shapes

R. J. Bieniek and T. J. Streeter

*Department of Physics, University of Missouri—Rolla, Rolla, Missouri 65401*

(Received 2 August 1983)

When two atoms are in proximity, their resonance lines are broadened because of the formation of molecular potentials, between which photon transitions can occur. The level of experimental refinement in measuring excimer and collisional far-wing spectra calls for interpretive theoretical methods that accurately treat the observed structure in line shapes. Of particular interest are satellites and undulations, for they can give much information on intermolecular potentials. We derive an expression for  $T$ -matrix elements, based on JWKB wave functions and stationary-phase techniques, that is universally applicable to situations with one, two, or more Condon points. Each transition point is treated individually, with effects of potential shape, wave-function phases, and interference separately highlighted. The expression is tested against quantum-mechanical line shapes of the red and blue wings of the Rb  $D$  lines broadened by Xe perturbers. Agreement is quite good for both the red-wing undulations and the blue-wing satellite-supernumerary structure.

### I. INTRODUCTION

A number of interesting spectral features have been observed in excimer spectra and in the far wings of collisionally broadened atomic lines, particularly undulations and satellite peaks.<sup>1-3</sup> Such structure is particularly evident in the experimental line shapes obtained by Sayer *et al.* for collisionally induced dipole absorption in the far wings of the dipole-forbidden  $6S_{1/2} \rightarrow 5D_{5/2}$  line of Cs.<sup>4</sup> Very analogous structures have been observed in the energy spectra of electrons ejected in Penning ionization.<sup>5</sup> These can be understood in the context of free-free, free-bound, or bound-free transitions between the molecular or quasistatic potentials. Advanced stationary-phase techniques,<sup>6-10</sup> based on JWKB wave functions, have been used to explain the existence of these features through an analysis of the distorted-wave integral for the  $T$ -matrix element

$$T_{fi}(\epsilon) = \int_0^\infty \psi_f(R)t(R)\psi_i(R)dR. \quad (1)$$

Here,  $\epsilon = h\nu$  is the energy of the photon,  $R$  is the internuclear separation of the colliding atoms, the  $\psi_i(R)$  and  $\psi_f(R)$  are initial and final distorted radial wave functions, and  $t(R)$  is the electronic transitional coupling amplitude. [In the case of collisional far-wing line broadening,  $t(R)$  is the transition dipole moment.] The integrand in Eq. (1) generally oscillates rapidly, and little contribution occurs. The main contributions to the integral arise where the integrand is slowly varying. This occurs at stationary-phase points, which correspond to the Condon points for vertical transitions in the simple semiclassical description.<sup>6-11</sup> Quantum-mechanical computations have explicitly demonstrated that the major contributions to  $T_{fi}$  come from values of  $R$  near a Condon point.<sup>12,13</sup>

Experimental work<sup>2-4</sup> is at a level of refinement that calls for interpretive, utilitarian theories that accurately account for the positions and amplitudes of the peaks and undulations in far-wing line shapes. Quantum-mechanical

computations can produce accurate line shapes for known potentials. However, it is difficult to determine potentials from experimental spectra when the separate causes for far-wing structure are buried in quantal numerics. What is desired is a theoretical expression that is quantitatively accurate, yet qualitatively sorts out the effects of initial and final wave-function phases at the transition points, shapes of intermolecular potentials, and interference among Condon points. This paper develops and tests such an expression, obtained from stationary-phase techniques. It can be applied to situations with one, two, or even more Condon points.

### II. Rb\* + Xe AS AN ILLUSTRATIVE SYSTEM

To illustrate and examine the phenomena described above, we will consider the emission spectra in the far wings of the Rb  $D$  lines broadened by Xe perturbers. The wings are produced by photon-emitting electronic transitions that occur between the quasistatic potentials that form during a collision. The wing-emission line shape (total emission rate of photon energy per unit frequency interval per unit densities of the colliding species) is<sup>8</sup>

$$I_\nu = \frac{dI}{d\nu} = (1024\pi^5\mu c/3\hbar k_i)\lambda^{-4} \sum_l (2l+1) |T_{fi}^l|^2, \quad (2)$$

where  $\nu$  is the frequency of a photon and  $\lambda$  its wavelength.  $\mu$  is the reduced mass of the colliding atoms,  $k_i$  is the wave number of their initial relative motion, and  $l$  is the quantum number of the  $l$ th partial wave. Interesting structure has been experimentally resolved in these wings.<sup>2,3</sup> The red wing of the Rb  $D_1$  line ( $5^2P_{1/2} \rightarrow 5^2S_{1/2}$ , 7947 Å) is produced by transitions from the  $A^2\Pi_{1/2}$  excited-state potential to the  $X^2\Sigma_{1/2}$  ground-state potential. The blue wing of the  $D_2$  line ( $5^2P_{3/2} \rightarrow 5^2S_{1/2}$ , 7800 Å) is caused by transitions from the  $B^2\Sigma_{1/2}$  state to the  $X^2\Sigma_{1/2}$  state. Figure 1 schematically illustrates the general form of these potentials. Fig-

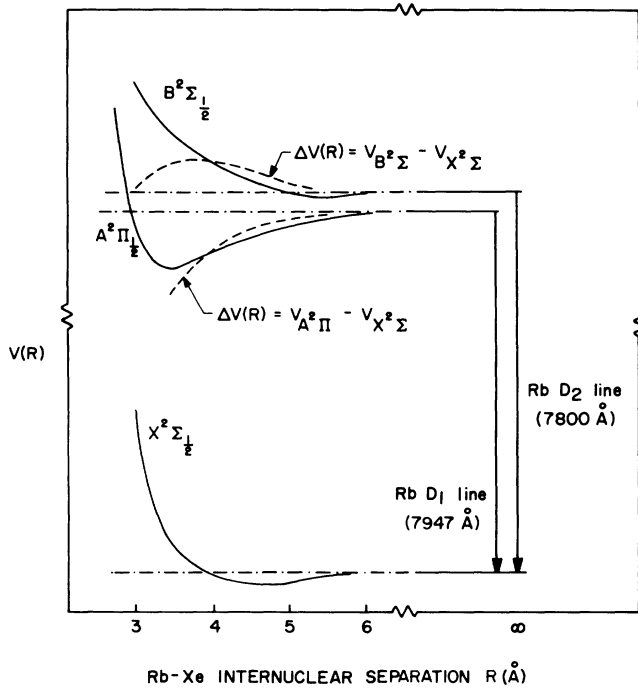


FIG. 1. Schematic diagram of the quasistatic potentials associated with the broadening of the Rb  $D$  lines by Xe perturbers. (An  $A^2\Pi_{3/2}$  state is not shown.)

ure 2 displays the results of a quantum-mechanical calculation for the contribution to the red-wing line shape from a single representative collisional energy in the thermal range. Figure 3 displays an analogous calculation for the blue wing. The quantum-mechanical techniques for computing these line shapes are described elsewhere.<sup>9</sup>

The potentials actually used to generate these line shapes are modified versions of semiempirical<sup>3,8</sup> and *ab initio*<sup>14</sup> potentials. The precise nature of the potentials need not be reported here because the accuracy of stationary-phase methods is to be tested, not the potentials. The approximations should be tested against quantal calculations using the same set of selected potentials, and not compared to experimental results that requires knowledge of the true potentials. (As it is, though, the computed red wing is in good agreement with experiment, and the blue wing is in fair agreement.) In all calculations, the dipole transition moment was assumed to be constant at all  $R$  to focus on the effects of potentials and wave functions. This is why the intensity scale is arbitrary, though linear.

### III. STATIONARY-PHASE EVALUATION OF THE $T$ MATRIX

For a particular distorted-wave channel  $a$ , the simple JWKB wave function associated with total energy  $E_a$  is given by

$$\psi_a(R | E_a) = A_a(R | E_a) \sin[\phi_a(R | E_a)], \quad (3a)$$

where the amplitude, phase, and local wave number are

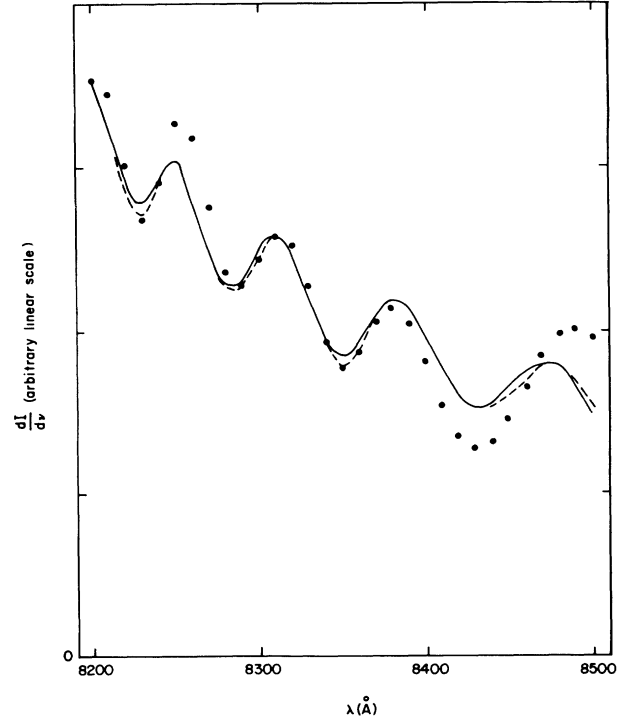


FIG. 2. Computed emission spectrum of the far red wing of the Rb  $D_1$  line (7947 Å) broadened by Xe perturbers for a collisional energy of 0.01 eV. — quantum mechanical; - - - stationary phase using  $F(y) = \text{Bi}(y)$  or  $F(y) = -|y|^{-1/4} \text{Ai}'(y)$  in Eq. (10); ··· stationary phase using  $F(y) = \text{Gi}(y)$  in Eq. (10).

$$A_a(R | E_a) = k_a^l(R | E_a)^{-1/2}, \quad (3b)$$

$$\phi_a(R | E_a) = \int_{R_a^l}^R k_a^l(r | E_a) dr + \frac{1}{4}\pi, \quad (3c)$$

$$k_a^l(R | E_a)^2 = \frac{2\mu}{\hbar^2} [E_a - V_a(R)] - \frac{(l + \frac{1}{2})^2}{R^2}. \quad (3d)$$

$V_a(R)$  is the intermolecular potential, and  $R_a^l(E_a, l)$  is the classical turning point defined by  $k_a^l(R_a^l | E_a) = 0$ . The parametric dependence of these functions on  $E_a$  and collisional angular momentum quantum number  $l$  will not be explicitly indicated in the discussion below, but should be implicitly understood.

Using Eqs. (1)–(3), we find

$$T_{fi}(\epsilon) \approx \frac{1}{2} \int f(R) \cos[\Delta\phi(R)] dR, \quad (4a)$$

where

$$\Delta\phi(R) = \phi_f(R) - \phi_i(R), \quad (4b)$$

$$f(R) = t(R) A_i(R) A_f(R). \quad (4c)$$

$f(R)$  will usually vary much more slowly than  $\cos[\Delta\phi(R)]$  in  $T_{fi}$ . The major contributions to  $T_{fi}$  will come from values of  $R$  near the points of stationary phase  $R_c$  where the cosine factor is also slowly varying. These satisfy  $\Delta\phi'(R_c) = 0$ . This condition immediately implies that the local nuclear kinetic energy and electronic energies are separately conserved at the Condon points, i.e.,  $k_i(R_c) = k_f(R_c)$  and  $\epsilon = \Delta V(R_c) = V_i(R_c) - V_f(R_c)$  where

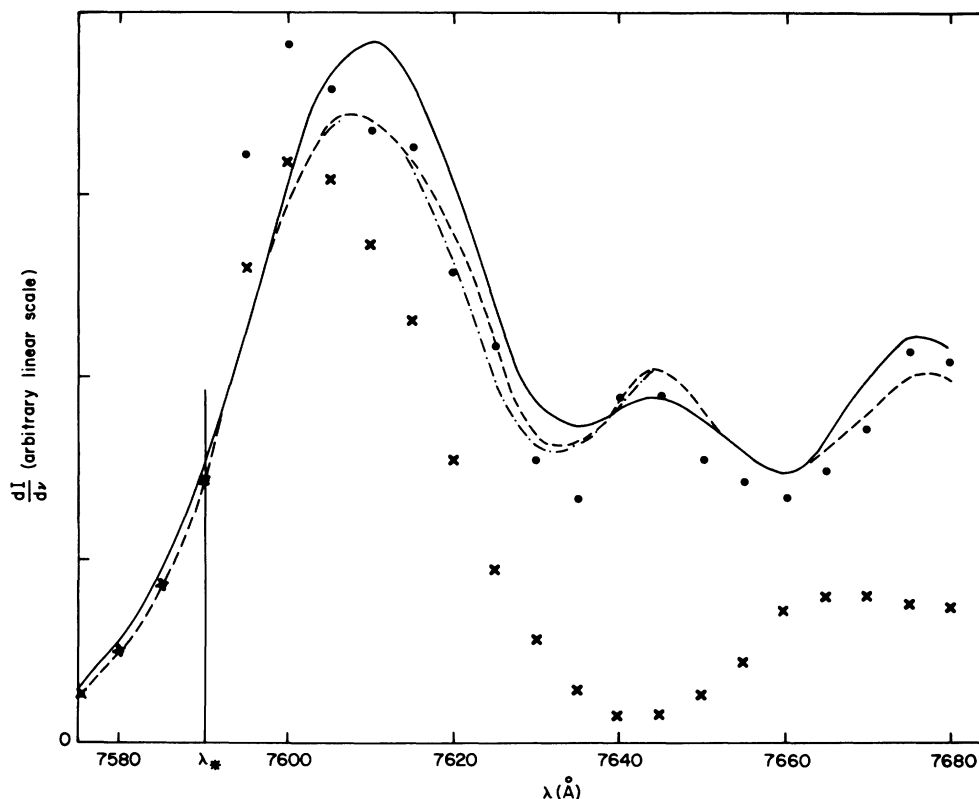


FIG. 3. Computed emission spectrum of the far blue wing of the Rb  $D_2$  line (7800 Å) broadened by Xe perturbors. — quantum mechanical; - - - stationary phase using  $F(y)=\text{Bi}(y)$  in Eq. (10); ··· stationary phase using  $F(y)=\text{Gi}(y)$  in Eq. (10); ××× straightforward Sando-Wormhoudt formula [Eq. (15)]; -·- partial Sando-Wormhoudt technique [Eq. (16)].

$\epsilon$  is the energy of the far-wing photon.<sup>6</sup> Note that the asymptotic value for the potential difference  $\Delta V(\infty)$  is the energy of the atomic resonance line.

Much attention has been given to processes involving an extremum in the difference potential  $\Delta V(R)$ . This means there can be two Condon points,  $R_1$  and  $R_2$ , which satisfy

$\epsilon = \Delta V(R_c)$ . The ir caustic coalescence for photon energies near the extremum produces a satellite peak in a far-wing line shape.<sup>6,15</sup> Stationary-phase methods have been developed to evaluate  $T_{fi}$  analytically in ways that remain uniformly applicable whether  $R_1$  and  $R_2$  are close to or far from one another.<sup>16-18</sup> They have the form

$$T_{fi}(\epsilon) \simeq (\pi/\sqrt{2})\rho(R_1, R_2)^{1/4} [(\beta_1 + \beta_2)\cos(\xi(R_1, R_2))\text{Ai}(-\rho(R_1, R_2)) - (s_1\beta_1 + s_2\beta_2)\sin(\xi(R_1, R_2))F(-\rho(R_1, R_2))], \quad (5a)$$

where

$$\xi(R_1, R_2) = \frac{1}{2}[\Delta\phi(R_1) + \Delta\phi(R_2)], \quad (5b)$$

$$\rho(R_1, R_2) = \left\{ \frac{3}{4}[s_1\Delta\phi(R_1) + s_2\Delta\phi(R_2)] \right\}^{2/3}, \quad (5c)$$

$$s_c = \Delta\phi''(R_c) / |\Delta\phi''(R_c)|^{-1}, \quad (5d)$$

$$\beta_c = f(R_c) / |\Delta\phi'''(R_c)|^{-1/2}. \quad (5e)$$

Note  $s_1 = -s_2$ . Different analytic methods give related, but different versions of  $F(-\rho)$ . The possibilities are

$$F(-\rho) = \begin{cases} \text{Bi}(-\rho), & \text{from Ref. 16,} & (6a) \\ \text{Gi}(-\rho), & \text{from Ref. 17,} & (6b) \\ -\rho^{-1/2}\text{Ai}'(-\rho), & \text{from Ref. 18.} & (6c) \end{cases}$$

Here,  $\text{Ai}(-\rho)$  is the regular homogeneous Airy function,  $\text{Bi}(-\rho)$  is the irregular homogeneous Airy function, and  $\text{Gi}(-\rho)$  is the regular inhomogeneous Airy function.<sup>19</sup>

All forms of  $F(-\rho)$  yield the same values for  $T_{fi}$  in limiting cases of  $R_1$  and  $R_2$  either very close together or very far apart. Which choice is numerically most accurate in the more usual, intermediate situation will be examined in Sec. IV.

Actual wing spectra may be associated with one, two, or more Condon points (in cases, respectively, of difference potentials with no,<sup>3</sup> one,<sup>2</sup> or more<sup>20</sup> extrema). Thus, it would be useful to have an expression that is universally applicable for any number of stationary-phase points, satisfying  $\epsilon = \Delta V(R_c)$ . The approach we present below treats each point individually rather than in pairs.

To convert Eq. (5) into an expression useful for individual Condon points, we rearrange it into a form which begins to highlight the different points separately:

$$T_{fi}(\epsilon) = T_1(R_2) + T_2(R_1), \quad (7a)$$

where

$$T_c(R_n) = (\pi/\sqrt{2})\beta_c \rho(R_c, R_n)^{1/4} [\cos(\xi(R_c, R_n))\text{Ai}(-\rho(R_c, R_n)) - s_c \sin(\xi(R_c, R_n))F(-\rho(R_c, R_n))] . \quad (7b)$$

The influence of each Condon point on one another is still transmitted through  $\xi$  and  $\rho$ . This explicit mathematical association can be broken in a uniform way by making a cubic expansion of the phase change at each individual Condon point  $R_c$ . Noting that  $\Delta\phi'_c = 0$ , we have

$$\Delta\phi(R) \simeq \Delta\phi_c + \frac{1}{2}(R - R_c)^2 \Delta\phi''_c + \frac{1}{6}(R - R_c)^3 \Delta\phi'''_c , \quad (8)$$

where the subscript  $c$  implies evaluation of the derivatives at  $R_c$ . This expansion produces, for each  $R_c$ , an artificial, second stationary-phase point  $\bar{R}_c$  that also satisfies  $\Delta\phi'(\bar{R}_c) = 0$ . This is located at  $\bar{R}_c = R_c - 2\Delta\phi'''_c/\Delta\phi''_c$ .  $\{R_c, \bar{R}_c\}$  can be used as the pair of Condon points required to evaluate  $\xi$  and  $\rho$  in Eq. (6):

$$T_{fi}(\epsilon) \simeq T_1(\bar{R}_1) + T_2(\bar{R}_2) . \quad (9)$$

The explicit dependence of the Condon points on each other has been removed and each can be treated individually. Equations (5) and (9) agree when  $R_1$  and  $R_2$  are close together because the cubic expansions about each point will then be very nearly the same. When they are far apart ( $\xi$  large), they attain the same asymptotic expression even though the artificial stationary-phase points may not be near the actual ones. (This just means that the points do not “communicate” when they are far apart.)

What we have done in Eq. (9) is determine the contribution from individual points of stationary phase when a cubic fit is made to the phase change  $\Delta\phi(R)$  at a Condon point. We conclude that a general expression for  $T_{fi}$  with one or more Condon points can be obtained by simply adding their individual contributions:

$$T_{fi}^l(\epsilon) = \sum_c T_c^l(\epsilon) , \quad (10a)$$

where

$$T_c(\epsilon) = \frac{1}{2} \pi f_c \left| \frac{1}{2} \Delta\phi'''_c \right|^{-1/2} \times [\cos(u_c)\text{Ai}(y_c) - s_c \sin(u_c)F(y_c)] \quad (10b)$$

with

$$y_c = -\bar{\rho}(R_c, \bar{R}_c) = -\left(\frac{1}{2} \Delta\phi''_c\right)^2 \left| \frac{1}{2} \Delta\phi'''_c \right|^{-4/3} , \quad (10c)$$

$$u_c = \bar{\xi}(R_c, \bar{R}_c) = \Delta\phi_c + \frac{2}{3} s_c \left| y_c \right|^{3/2} . \quad (10d)$$

The bars over  $\rho$  and  $\xi$  indicate use of Eq. (8). This is the primary derivational result of this paper. This formula can be used no matter how many roots there are of  $\epsilon = \Delta V(R_c)$ . One excludes in Eq. (10a) any Condon point that is within the collisionally forbidden region inward of a turning point for higher values of angular momentum.

It can be shown that<sup>6</sup>

$$\Delta\phi'''_c \simeq \frac{\mu}{\hbar^2 k_c} \Delta V''_c \quad (11a)$$

and

$$y_c \simeq - \left[ \frac{2\mu}{\hbar^2 k_c} \right]^{2/3} (\Delta V'_c)^2 (2\Delta V''_c)^{-4/3} . \quad (11b)$$

These relations clearly show how Eq. (10b) relates  $T$ -matrix structure (and, thereby, line-shape structure) to the shape of intermolecular potentials through the derivatives of  $\Delta V(R)$ . The phases of the wave function then only appear in  $u_c$ . Thus, we have separated out the various sources of line-shape structure.

Before turning to numerical tests of Eq. (10), we must develop a way to handle transitions associated with a pair of complex Condon points. Such situations occur when the difference potential has an extremum, and we wish to consider transitions that emit photons with energies in the classically inaccessible dark side. Let  $R_*$  be the internuclear separation of an extremum in  $\Delta V(R)$ .  $\epsilon_* \equiv \Delta V(R_*)$  is often called the energy or “position” of the classical satellite. Near such a satellite, on its classically accessible side, there will be two real roots,  $R_1$  and  $R_2$ , of  $\Delta V(R_c) = \epsilon$ . For energies  $\epsilon$  on the dark side, there will be no real roots. However, we can determine dark side  $T$ -matrix elements by analytic continuation from the classically allowed case. When  $R_1$  and  $R_2$  are near coalescence ( $\epsilon \simeq \epsilon_*$ ),

$$u_2 = u_1 = \xi(R_1, R_2) = \Delta\phi \left[ \frac{1}{2}(R_1 + R_2) \right] = \Delta\phi(R_*) \equiv \Delta\phi_* \quad (12)$$

and

$$\begin{aligned} y_2 &= y_1 \\ &= - \left[ \frac{2\mu}{\hbar^2 k_*} \right]^{2/3} (s \Delta V''_*)^{-1/3} (\epsilon - \epsilon_*) \\ &\equiv y_*(\epsilon) , \end{aligned} \quad (13)$$

where  $k_* = k(R_*)$  and  $\Delta V''_* = \Delta V''(R_*)$ . The branch of the third-root in Eq. (13) is chosen such that it has the same sign as  $\Delta V''(R_*)$ , ensuring  $y < 0$  for classically accessible transitional energies  $\epsilon$ . To include dark-side transitions beyond the classical satellite, we just use Eq. (13) to carry us there. Using the fact that  $s_1 = -s_2$ , we find that a  $T$ -matrix element for a pair of Condon points associated with either classically allowed or disallowed transitions near the satellite is

$$T_{\text{sat}}(\epsilon) \simeq \pi f_* \left| \frac{\mu \Delta V''_*}{2\hbar^2 k_*} \right|^{-1/2} \cos(\Delta\phi_*) \text{Ai}(y_*(\epsilon)) . \quad (14)$$

This should be valid for situations in which  $f(R_1) \simeq f(R_2) \simeq f_*$  and the difference potential is effectively quadratic between  $R_1$  and  $R_2$ .

Equation (14) is the foundation of the Sando-Wormhoudt formulas that have become popular means of deducing excited-state potentials from experimental spectra.<sup>3,6,21</sup> Building upon this approximation, one concludes that, for a thermal distribution, the satellite energy  $\epsilon_*$ , and thus the extremum value in the difference potential  $\Delta V(R)$ , is easily found on the dark side of the satellite

peak at a position of 65% of the maximum intensity.<sup>3</sup> The exponential falloff of the intensity on the darkside has been commonly used to determine  $\Delta V^*$ .<sup>3,6</sup> Armed with this information, one can construct the difference potential near  $R_*$  and, from that, determine an excited-state potential if the lower one is known. In Sec. IV, we will examine the validity of these assumptions.

#### IV. RED- AND BLUE-WING TESTS

As discussed in Sec. II, the red wing of the Rb  $D_1$  line broadened by Xe perturbers is due to transitions between  $A^2\Pi_{1/2}$  and  $X^2\Sigma_{1/2}$  quasistatic potentials. The difference potential in this case is a monotonic function of internuclear separation. Hence, there is only a single solution of  $h\nu = \Delta V(R_c)$  for a given photon wavelength. The sum over Condon points in Eq. (10a) reduces to one term, given by Eq. (10b). This single Condon point produces no satellite peak, although prominent undulations are superimposed on a monotonic base. Figure 2 displays the results of using the three different forms of  $F(y)$  from Eq. (6) in Eq. (10). As can be seen, the choice  $F(y) = \text{Gi}(y)$  does not do as well as one would like if the extrema in the undulations are to be used in analyses.<sup>9</sup> Fortunately, both  $\text{Bi}(y)$  and  $-|y|^{-1/2}\text{Ai}'(y)$  do very well as  $F(y)$ .

Unlike the difference potential between the  $A^2\Pi_{1/2}$  and  $X^2\Sigma_{1/2}$  states, the one between the  $B^2\Sigma_{1/2}$  and  $X^2\Sigma_{1/2}$  states exhibits an extremum. For the numerical potentials employed in this study, the wavelength of the classical satellite is  $\lambda_* = hc/\epsilon_* = 7590 \text{ \AA}$ . For wavelengths shorter than the atomic  $D_2$  lines (7800 \AA), there are two Condon points that satisfy  $h\nu = \Delta V(R_c)$ . This double-point situation produces the blue-wing satellite shown in Fig. 3.

To compute the satellite line shape from the stationary-phase approach represented by Eq. (10), we had to consider the effects of collisional turning points on the transitions. This was not a serious issue for the red-wing calculation because the turning points were still far from the Condon points when an outer centrifugal barrier terminated the sum in Eq. (2) at  $l=110$ . However, at the higher energy used for the blue-wing calculation, such a cutoff does not occur. Instead, the turning points move outward as  $l$  increases, coming near and eventually containing the Condon points. The simple JWKB amplitudes and phases given by Eq. (3) are then no longer valid for use in Eq. (10). As described elsewhere, uniform amplitudes and phases can be employed for a Condon point that is in a classically allowed region, but near a turning point.<sup>9,22</sup> When it slips inside the turning point at high  $l$ , its contribution can be simply ignored in the sum over Condon points in Eq. (10a) because its contribution will be relatively small.

The results of using Eq. (10) to compute the blue-wing-satellite line shape are shown in Fig. 3. Again, the selection of  $F(y) = \text{Gi}(y)$  is not satisfactory while  $F(y) = \text{Bi}(y)$  does quite well.  $F(y) = -|y|^{-1/2}\text{Ai}'(y)$  gives a line shape of intermediate accuracy, and is not reported here. Because  $\text{Bi}(y)$  also did well for the red wing, we conclude that  $F(y) = \text{Bi}(y)$  is the best choice for use in Eq. (10b). This is the primary numerical conclusion of this paper.

#### V. SANDO-WORMHOUDT TECHNIQUES

One can use Eq. (14) to compute the intensity on both the bright side and dark side of a satellite. In keeping with the usual application of the Sando-Wormhoudt technique described at the end of Sec. III, the sum over angular momenta in Eq. (2) was approximated by

$$\sum_l (2l+1) |T_{fi}^l|^2 \simeq \sum_{l=0}^{l_*} (2l+1) |T_{\text{sat}}^l(\epsilon)|^2, \quad (15)$$

where  $l_*$  is the maximum  $l$  for which the satellite's  $R_*$  is collisionally accessible, i.e.,  $k_i^{l_*}(R_* | E_i) = 0$ . For a range of  $l$  just below  $l_*$ , both Condon points are assumed to contribute equally to the line shape, even though the inner one may be inside a collisional turning point and actually contributes little. The resulting line shape is shown in Fig. 3. The maximum and width of the satellite peak do not agree with quantal calculations. Furthermore, the first super-numerary oscillation from Eq. (15) is not located at the first undulation of the quantal results. This seriously calls into question the efficacy of analyses based on a straightforward application of the Sando-Wormhoudt approach.

We have found that the cause of the discrepancy is not Eq. (14) as such, but its indiscriminate use in Eq. (15). For  $l \leq 50$ , both Condon points associated with each wavelength in Fig. 3 are collisionally accessible. Up to this  $l$ , the numerical line shape obtained from Eq. (15) agrees very well with the quantal partial sum. For higher  $l$ , the turning points progressively pass the inner Condon points, with those from the longer wavelengths going first. It is for these higher  $l$  that the results from Eq. (15) begin to deviate from quantal results. We might expect, then, that one could use Eq. (14) when both Condon points are collisionally accessible, and Eq. (10b) when only the outer of the pair is. This means

$$\sum_l (2l+1) |T_{fi}^l(\epsilon)|^2 \simeq \sum_{l=0}^{l_1} (2l+1) |T_{\text{sat}}^l(\epsilon)|^2 + \sum_{l=l_1+1}^{l_2} (2l+1) |T_2^l(\epsilon)|^2, \quad (16)$$

where  $l_c$  is the maximum  $l$  for which penetration to  $R_c$  is classically possible. As shown in Fig. 3, there are no significant differences between the numerical results obtained from this equation and those from Eq. (10).

#### VI. CONCLUSIONS

Using JWKB and stationary-phase methods, we have derived an expression, Eqs. (10) with (6a), that can be used to calculate accurately the  $T$ -matrix elements for spectral transitions in the far wings of collisionally broadened lines. Each Condon point is treated individually, and the same formula can be used for cases of one, two, or more transition points. This can help elucidate the undulatory structure experimentally observed in far-wing line shapes. It can also be used to determine more accurately the differential absorption coefficients required in the analysis of polarization in collisionally redistributed atomic fluorescence.<sup>23</sup>

The good agreement between Eq. (16) and quantal calculations leads us to a number of conclusions of practical interest. The difference potential is effectively quadratic throughout the satellite and supernumerary regime. Because dark-side transitions are occurring semiclassically at a single, coalesced Condon point  $R_*$ , the common practice of determining the second derivative of the difference potential  $\Delta V''$  from the exponential decay of intensity is valid. However, for a pair of separated Condon points associated with the bright side, the outer of the two can contribute significantly to the line shape over a range of angular momentum that precludes collisional penetration to the inner point. This tends to make the satellite peak significantly broader than expected from a straightforward Sando-Wormhoudt analysis. This could lead to an error in determining the energy  $\epsilon_*$  of the classical satellite from

the 65% rule. Finally, not all of the prominent undulations near the satellite peak are the supernumerary oscillations associated with coalescing Condon points for difference potentials with extrema. In Fig. 3, the first undulatory peak at 7645 Å is due to single Condon points that are collisionally accessible at higher  $l$ . This secondary peak is then not a supernumerary as one might expect, but is rather more akin to the undulations arising in the red wing (Fig. 2) from a monotonic difference potential.

#### ACKNOWLEDGMENT

This work was supported by the Research Corporation under a Cottrell Research grant, and by the University of Missouri under a Weldon Spring grant.

- 
- <sup>1</sup>D. L. Drummond and A. Gallagher, *J. Chem. Phys.* **60**, 3426 (1974); R. Scheps, Ch. Ottinger, G. York, and A. Gallagher, *ibid.* **63**, 2581 (1975); M. C. Castex, *ibid.* **66**, 3854 (1977); R. J. Exton and W. L. Snow, *J. Quant. Spectrosc. Radiat. Transfer* **20**, 1 (1978); J. Tellinghuisen, G. Pichler, W. L. Snow, M. E. Hillard, and R. J. Exton, *Chem. Phys.* **50**, 313 (1980); M. C. Castex, M. Morlais, F. Spiegelmann, and J. P. Malrieu, *J. Chem. Phys.* **75**, 5006 (1981); R. Duren, E. Hasselbrink, H. Tischer, S. Milosevic, and G. Pichler, *Chem. Phys. Lett.* **89**, 218 (1982); T. Moeller, B. Jordan, P. Gurtler, G. Zimmerer, D. Hanks, J. Le Calve, and M. C. Castex, *Spectral Line Shapes* (Gruyter, New York, 1983), Vol. 2, p. 597; F. X. Gadea, F. Spiegelmann, M. C. Castex, and M. Morlais, *J. Chem. Phys.* **78**, 7270 (1983).
- <sup>2</sup>C. G. Carrington and A. Gallagher, *Phys. Rev. A* **10**, 1464 (1974).
- <sup>3</sup>C. G. Carrington and A. Gallagher, *J. Chem. Phys.* **60**, 3436 (1974).
- <sup>4</sup>B. Sayer, M. Ferray, J. P. Visticot, and J. Lozingto, *J. Phys. B* **13**, 177 (1980).
- <sup>5</sup>H. Morgner and A. Niehaus, *J. Phys. B* **12**, 1805 (1979).
- <sup>6</sup>K. M. Sando and J. C. Wormhoudt, *Phys. Rev. A* **7**, 1889 (1973).
- <sup>7</sup>J. Szudy and W. E. Baylis, *J. Quant. Spectrosc. Radiat. Transfer* **15**, 641 (1975).
- <sup>8</sup>R. J. Bieniek, *Phys. Rev. A* **15**, 1513 (1977).
- <sup>9</sup>R. J. Bieniek, *Phys. Rev. A* **23**, 2826 (1981).
- <sup>10</sup>R. J. Bieniek, *J. Phys. B* **7**, L266 (1974).
- <sup>11</sup>A. Jablonski, *Phys. Rev.* **68**, 78 (1945).
- <sup>12</sup>C. Noda and R. N. Zare, *J. Mol. Spectrosc.* **95**, 254 (1982).
- <sup>13</sup>J. Tellinghuisen, *Bull. Am. Phys. Soc.* **28**, 791 (1983).
- <sup>14</sup>W. E. Baylis, private communication.
- <sup>15</sup>R. E. M. Hedges, D. L. Drummond, and A. Gallagher, *Phys. Rev. A* **6**, 1519 (1972).
- <sup>16</sup>W. H. Miller, *J. Chem. Phys.* **53**, 3578 (1970); **54**, 5386 (1971).
- <sup>17</sup>R. J. Bieniek, *Chem. Phys. Lett.* **40**, 72 (1976).
- <sup>18</sup>J. N. L. Connor, *Mol. Phys.* **25**, 181 (1973).
- <sup>19</sup>*Handbook of Mathematical Functions*, edited by M. Abramowitz and I. A. Stegun, National Bureau of Standards Applied Mathematics Series, No. 55 (Dover, New York, 1965).
- <sup>20</sup>J. Lorenzen and K. Niemax, *Z. Naturforsch. Teil A* **32**, 853 (1977); B. Cheron, R. Scheps, and A. Gallagher, *J. Chem. Phys.* **65**, 326 (1976).
- <sup>21</sup>For example, see Duren *et al.* in Ref. 1; J. P. Visticot, J. Szudy, M. Ferray, and B. Sayer, *J. Phys. B* **14**, 2329 (1981); **14**, 4755 (1981).
- <sup>22</sup>R. J. Bieniek, *J. Chem. Phys.* **72**, 1225 (1980); **73**, 4712(E) (1980).
- <sup>23</sup>J. L. Carlsten, A. Szöke, and M. G. Raymer, *Phys. Rev. A* **15**, 1029 (1977); E. L. Lewis, M. Harris, W. J. Alford, J. Copper, and K. Burnett, *J. Phys. B* **16**, 553 (1983).